

# Design and Optimization of Heat-Integrated Distillation Column Schemes through a New Robust Methodology Coupled with a Boltzmann-Based Estimation of Distribution Algorithm

Roberto Gutiérrez-Guerra,<sup>†</sup> Jazmin Cortez-González,<sup>†</sup> Rodolfo Murrieta-Dueñas,<sup>†</sup> Juan Gabriel Segovia-Hernández,<sup>\*,†</sup> Salvador Hernández,<sup>†</sup> and Arturo Hernández-Aguirre<sup>‡</sup>

<sup>†</sup>Departamento de Ingeniería Química, Universidad de Guanajuato, Campus Guanajuato, Noria Alta s/n, 36050, Guanajuato, Guanajuato, Mexico

<sup>‡</sup>Departamento de Computación, Centro de Investigación en Matemáticas, A.C., A.P. 402, Guanajuato, Guanajuato, CP 3600, México.

**ABSTRACT:** The technology of the heat-integrated distillation column (HIDiC) has shown to be a potential energy-saving alternative for separating close-boiling mixtures. However, the economic aspects are a critical factor to extensive use of this distillation sequence in real applications. In this research, a novel stochastic optimization algorithm called Boltzmann univariate marginal distribution algorithm (BUMDA) with constraints handling has been implemented to optimize HIDiC sequences. Three binary mixtures were examined: butanol–isobutanol, *n*-heptane–cyclohexane, and benzene–toluene. The evaluation was performed by applying a new robust methodology using the interface Matlab–Excel–Aspen Plus. The model Radfrac was used in the simulations in Aspen Plus. The minimization of the total annual cost was established as the fitness function of the problem. Results showed the great robustness presented by the BUMDA algorithm for solving successfully this kind of complex optimization problem. Thus, the HIDiC design to separate the alcohol mixture showed energy savings of 84% and a cost that was lower (2%) than that of the conventional column. In addition, the hydrocarbon mixtures reached energy savings of 62.5% (*n*-heptane–cyclohexane) and 52.5% (benzene–toluene). Nevertheless, the total annual cost (TAC) of the HIDiC is larger than the TAC of the conventional column (32% and 35%, respectively).

## 1. INTRODUCTION

Distillation is a fundamental operation in the chemical process industries because this technology is used to split around 95% of the fluids in this sector. However, this wide application has led to the use of large amounts of energy because the operational principle of this technology is based on the addition (in the reboiler) and elimination (in the condenser) of heat. Regarding distillation, it is considered that 3% of the world's energy is used for this separation technology<sup>1,2</sup> as a result of its low thermodynamic efficiency (5–20%),<sup>3,4</sup> representing 70% of the total annual costs; in addition, it has large environmental footprint of carbon dioxide because the heat is generated by the burning of fossil fuels. With the goal of enhancing the thermodynamic efficiency, economy, and environmental impact of the distillation systems, diverse technologies have been presented, such as configurations with interboilers and intercondensers, heat pump systems,<sup>5–8</sup> multieffect columns,<sup>9–12</sup> thermally coupled sequences,<sup>13</sup> and recently the internally heat-integrated distillation columns HIDiC.<sup>14–18</sup> In particular, HIDiC configurations have shown great potential energy savings compared with other technologies, especially splitting close boiling mixtures, dividing the conventional column into its corresponding rectifying and stripping sections, and generating temperature feasible driving forces between two sections (applying pressure changes) and transferring internal heat from the rectifying section (high pressure) to stripping section (low pressure).

The concept that supports the performance of the HIDiC was proposed originally in 1958 by Haselden for gas separation, and later the idea was reintroduced as the secondary reflux vaporization (SRV) method.<sup>19</sup> Also, to translate the concept toward physical design, a concentric heat-integrated column was invented, placing the annular stripping section around the rectifying section, which allowed the enhancement of the thermodynamic efficiency.<sup>20–22</sup> In other studies,<sup>23,24</sup> the separation of a benzene–toluene mixture using the HIDiC column was performed; the results showed energy savings around 30%. In addition, the principles of the HIDiC were applied to the cryogenic distillation column<sup>25</sup> using two small columns placed one above another to reduce the energy cost. Later, it was established that the HIDiC sequence led to energy savings of 50% compared with the vapor recompression column (VRC). At the same time, both the design complexity and the capital investment were analyzed.<sup>26</sup> Furthermore, a concentric column equipped with heat-transfer panels was patented.<sup>27</sup> In this column, panels were placed in the stripping and rectifying sections, which allowed flexible heat-transfer areas. Later, the HIDiC sequence was compared with the vapor recompression column to split the binary mixture propane–propylene.<sup>28</sup> Results presented revealed that the HIDiC was 14% cheaper

**Received:** January 7, 2014

**Revised:** June 5, 2014

**Accepted:** June 11, 2014

**Published:** June 11, 2014

than the VRC. Later, several HIDiC alternatives with different energy integration degrees were compared with the conventional system.<sup>29</sup> In that study it was shown that the intensified HIDiC is the most energy-efficient configuration. Nevertheless, through a closed loop controllability study<sup>30</sup> it was found that to split ternary mixtures, the intensified HIDiC presented properties that were worse than those of the ideal HIDiC (i-HIDiC) and the general HIDiC. In another study,<sup>31</sup> the thermodynamic feasibility of integrating energy under the pinch point concept was analyzed. Through this study was identified the minimum driving temperature to achieve heat integration to separate a mixture of benzene and toluene. Simultaneously, a hydraulic analysis in the physical configuration of the HIDiC was presented. In addition, HIDiC columns were used to separate two ternary mixtures made up of benzene/toluene/*p*-xylene and *n*-pentane/cyclopentane/2 methyl-heptane.<sup>32</sup> The application of this technology led to the achievement of energy savings of 30% and 50% for the respective mixtures. Later, the operational feasibility of the HIDiC column for splitting an aromatic mixture (benzene, toluene, *p*-xylene) via extractive distillation was presented.<sup>33</sup> The authors concluded that the HIDiC is the best option, compared with the Petlyuk column and the conventional sequence. Later, the great composed curved of the column was used to evaluate the thermodynamic potential of the HIDiC sequence for reducing the energy consumption in the separation of hydrocarbon ternary mixtures.<sup>34</sup> Results showed that these technologies are good options for reducing the energy consumption and reducing CO<sub>2</sub> emissions; however, it was concluded also that most of the HIDiC schemes are more expensive than the conventional configuration. Recently, an optimization study<sup>35</sup> was developed to analyze the performance of the HIDiC to fractionate two binary mixtures made up of benzene–toluene and propane–propylene. Two landscapes were taken into account: uniform heat distribution and uniform heat-transfer areas. Results for benzene–toluene showed that the optimum HIDiC structure was the structure with uniform heat-transfer area, with only one heat-integrated stage in each extreme of the column. Additionally, for the case of propane–propylene, the best design was that with uniform heat transfer integrating only the upper part of the top section of the column. In addition, an optimization via mixed integer nonlinear programming (MINLP) was used to determine the benefits of the HIDiC sequence considering the properties of the mixtures.<sup>36</sup> Results indicated that the HIDiC sequence is more favorable in energetic and economic terms at low relative volatility (<1.8). However, it is important to take into consideration that these results were obtained considering ideal thermodynamics (using Antoine's equation and Raoult's law) and do not take into account the nonlinear influence of heat exchanger cost, temperature bounds of utilities, and the influence of pressure on the capital cost.

To clarify the different HIDiC sequences mentioned above, they are presented in Figures 1–4.

First, the well-known conventional column to separate a binary mixture is presented, which includes the feed (F) that will be separated into two fractions, the distillate (D), and the bottoms (B). Next, this conventional column is divided into two symmetric columns, separating the rectifying section (SR) from the stripping section (SS) and connecting them through a compressor (C) and a throttling valve (TV) to give place to the HIDiC configurations.

The general HIDiC or simply HIDiC is termed the configuration with partial energy integration, i.e., it preserves

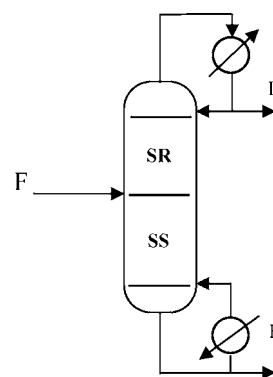


Figure 1. Conventional column.

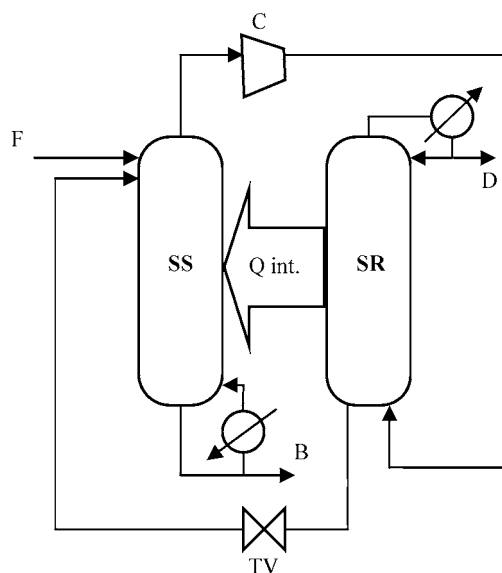


Figure 2. General HIDiC sequence.

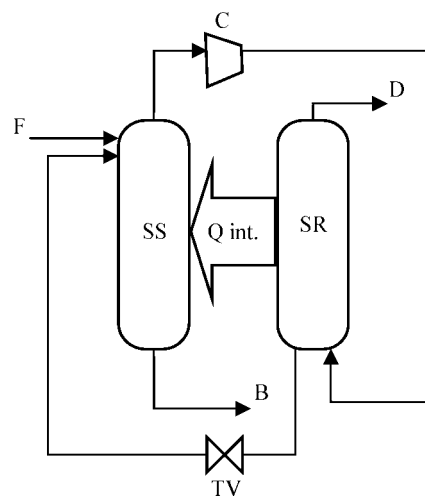


Figure 3. Ideal HIDiC sequence.

both the reboiler and condenser in its structure. In addition, the ideal HIDiC, is defined as the HIDiC configuration able to achieve the separation using only the energy internally integrated. This means that it is able to operate without reboiler or condenser after the start-up stage. Finally, the intensified HIDiC is formed by the ideal HIDiC, but at the

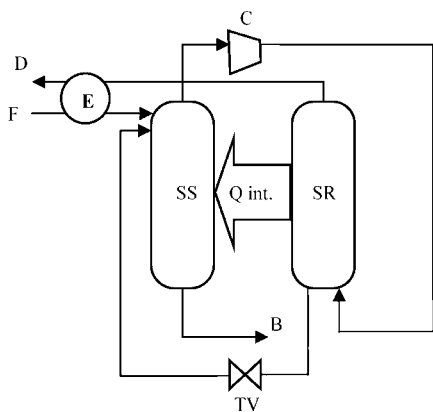


Figure 4. Intensified HIDiC sequence.

same time, this structure provides a portion of the energy contained in the distillate to preheat the feed of the stripping column through the exchanger (E). For the HIDiC configurations, the quantity of energy internally integrated is termed  $Q_{int}$ .

Therefore, with the goal of designing more efficient processes and obtaining more environmentally friendly separation technologies, the contribution (novelty) derived from this work is based on the following:

1. Using a constrained stochastic optimization algorithm attached with a reset mechanism to perform intensified searches. The intensification is translated as a way to frequently explore all search space. This exploration is performed when the reset mechanism is activated. The activation of the mechanism takes place when the variance is lower than a defined value, in this case 0.001.
2. Implementation of a robust methodology that leads to the evaluation of diverse energy integration degrees at each HIDiC design (individual) of the population. Through this strategy, a more detailed exploration is achieved and refined solutions are obtained.
3. Establishing the reflux ratio as an additional optimization variable in the HIDiC columns. This variable was included because in the methodology established it contributes to the determination of the amount of energy integrated between SR and SS. Thus, a convenient value for the reflux ratio must be obtained.

## 2. OPTIMIZATION TOOLS

The multivariable and highly nonlinear model in the distillation systems frequently have been solved through the mixed integer nonlinear programming (MINLP) to find the global optimum;<sup>36–40</sup> nevertheless, it is considered that these strategies disclose several difficulties around the exhaustive mathematical treatment of the fitness function when the complete modeling is included. Also, the convergence depends strongly on good initial guesses.

Other strategies widely used nowadays are those classified as stochastic methods, which do not guarantee finding the global optimum, but instead deal directly with the complete rigorous modeling of the process. The fitness functions can be explicitly described, or it can be conveniently treated as a black box, giving as a result a series of local optima that form a Pareto front of the contradicting fitness functions of the problem. The stochastic methods frequently applied to chemical processes that can be mentioned are the genetic algorithms,<sup>41</sup> differential

evolution,<sup>42</sup> and harmony search.<sup>43</sup> However, recently an algorithm called the Boltzmann univariate marginal distribution algorithm (BUMDA) was developed.<sup>44</sup> This algorithm has demonstrated great efficacy and robustness for optimizing considerably complex problems in chemical engineering.<sup>45</sup>

In this work, the Pareto set can be described in terms of the total annual cost (TAC), energy consumption in the reboiler, and carbon dioxide emissions. This comparison is proposed in order to determine simultaneously the most suitable balance between the total annual cost, energy consumption, and carbon dioxide emissions.

On the other side, taking into consideration that the energy consumption and the carbon dioxide emissions undergo a proportional behavior, both objectives can be represented simply by the energy consumption.

Thus, the TAC and the energy consumption represent conflicting objectives because a reduction of the energy consumption is commonly compensated by higher capital and electricity costs, which leads to obtain a higher TAC for the HIDiC.

In terms of the optimization variables, the conflict between the TAC and the energy consumption is produced because a superior reduction of the energy consumption means higher compression ratio (CR) and reflux ratio (RR) values to perform the energy integration. Consequently, with the increasing of CR and RR, a larger TAC is obtained as a consequence of the increasing capital and electricity costs.

On the other side, the choice of the BUMDA algorithm as optimizer of the HIDiC configurations was determined under a comparison with other stochastic methods (EMNA-B, BG-UMDA) to optimize several problems (Rosenbrock, Griewangk, sphere, parabolic ridge, sharp ridge, among others).<sup>44</sup> These problems are the common benchmark problems and represent considerable difficulties in finding the optimum. In several cases, the BUMDA algorithm showed a performance better than the that of other algorithms. Furthermore, in the worst situation, this algorithm was able to achieve a comparable performance in relation with the other strategies. In addition, it is important to mention that the problems were analyzed considering multiple dimensions (degrees of freedom), for instance 10, 50, and 80 dimensions. In literature related to the optimization using stochastic methods, a larger number of dimensions can be found. So, until now, it is observed that the dimensionality does not represent a drawback for these optimization strategies.

**2.1. Fundamentals of the BUMDA Algorithm.** The BUMDA is an algorithm belonging to the estimation of distribution algorithms (EDAs). These algorithms were derived from the genetic algorithms. The main difference among them is the method of generating the population. In genetic algorithms, each population is obtained using factors of mutation and crossing on the individuals with the best aptitude. In EDAs, a probability distribution is used to sample new candidate individuals. Thus, the probability distribution will determine which individuals must be considered to produce the next generation. For instance, for a problem of maximization, there will be a high probability of sampling individuals with the highest fitness function, and each new population is obtained employing these individuals. Therefore, all new individuals will be found around the maximum of the function. Otherwise, if the fitness function of the problem represents a minimization, the probability of sampling will be high on the region with the lowest values of the fitness function. Therefore, the new

population will meet the characteristics of the individuals with lowest fitness function.

With the aim of effectively guiding the convergence toward the optimum value, the BUMDA algorithm is supported by two key items: (1) the Boltzmann distribution and (2) the application of a truncation method of population on the best individuals.

**2.2. Boltzmann Distribution.** On one hand, the goal of the Boltzmann distribution is getting a continuous approximation to the fitness function ( $g(x)$ ) through the probability model ( $P(x)$ ) presented in eq 1. This means that the distribution is able to adapt to the function's shape and distinguish every optimum present on it.

Boltzmann distribution includes the fitness function, the parameter  $\beta$ , and the parameter of normalization  $Z$ . In the original context of the Boltzmann distribution,  $\beta$  is defined by the inverse product between the Boltzmann's constant ( $k$ ) and the temperature ( $T$ ),  $1/(kT)$ ; nevertheless, for EDAs, this parameter has a direct relationship with the selection pressure and the variance. Besides, the  $Z$  parameter is evaluated by the summation of the exponential function of the numerator, on the whole search domain, as it is indicated by eq 2.

$$P(x) = \frac{\exp[\beta g(x)]}{Z} \quad (1)$$

$$P(x_i) = \frac{\exp[\beta g(x_i)]}{\sum_x \exp[\beta g(x)]} \quad (2)$$

Boltzmann distribution involves using an infinite population in order to explore the complete search space of the function, but it does not represent an efficient way to carry out the exploration. Thus, the Boltzmann distribution has been approached by a normal distribution,  $Q(x)$ , represented by a Gaussian distribution, whose form is shown in eq 3. This distribution is properly defined as a function of the mean ( $\mu$ ) and variance ( $\nu$ ) of the population; the relationship with the Boltzmann distribution is determined by the Kullback–Leibler divergence (KLD). This divergence represents the distance or deviation between the Boltzmann and the normal distribution, such as it is observed in eq 4. Consequently, the minimization of KLD is achieved between the distributions in order to preserve the Boltzmann distribution essence using a low computational effort. Through the minimization and under several considerations along the mathematical treatment, were obtained the functions to evaluate both the mean and the variance of the population, which preserve the corresponding interrelation between both distributions. Thus, these variables will be computed and used to evaluate the normal distribution employed as the approximation. The corresponding expressions are represented by eq 5 and eq 6, respectively.

$$Q(x) = \prod_{i=1}^n Q_i(x) \quad \text{where}$$

$$Q_i(x) = Q_i(x_i, \mu_i, \nu_i) = \frac{\exp[-(x_i - \mu_i)^2 / 2\nu_i]}{(2\pi\nu_i)^{1/2}} \quad (3)$$

$$K_{Q,P} = \int_x Q_x \log \frac{Q_x}{P_x} dx \quad \text{naming } P(x) = P_x$$

$$\text{and } Q(x, \mu, \nu) = Q_x \quad (4)$$

$$\mu = \sum_{x_j} w(x_j)x_j \quad \text{defining } w(x_j) = \frac{g(x_j)}{\sum_{x_j} g(x_j)} \quad (5)$$

$$\nu = \sum_{x_j} w'(x_j)(x_j - \mu)^2 \quad \text{considering } w'(x_j) = \frac{g(x_j)}{\sum_{x_j} g(x_j) + 1} \quad (6)$$

Where  $x_j$  represents each individual selected.

**2.3. Truncation Method.** As can be seen in Figure 5 (for the case of a maximization problem), by means of truncation of

Truncation Method	
1.	For the initial population (t=0): Evaluate $g(x_i, 0)$ for $i=1..N$ Order the population in decreasing order Define: $\theta_0 = \min g(x_i, 0)$
2.	For $t > 0$ , do: $\theta_t = \max(\theta_{t-1}, \min(g(x_i, t)   g(x_i, t) \geq \theta_{t-1}))$
3.	If for the individuals ordered in decreasing order $g(x_{N/2}) \geq \theta_t$ , do: $\theta_t = g(x_{N/2})$ Where $N$ is the population size
4.	Truncate the population on $g(x_i, t) \geq \theta_t$ Where $x_i$ are all the individuals whose objective values are equal or greater than $\theta_t$

Figure 5. Truncation method in the BUMDA algorithm.

the population ( $\theta$ ) the fitness function on each generation follows an increasing behavior or at least is preserved on the best value obtained previously. Under this condition,  $\theta_t \geq \theta_{t-1}$ . Consequently, because the mean of the fitness function of the chosen set is limited by the aptitude value of the elite individual, the mean converges to it.

To provide a better understanding about the operation of the truncation method, it was graphically analyzed.<sup>44</sup> In the analysis, the value of the truncation was augmented from  $-0.7$  to  $1.2$ . The results show that as the truncation value increases, Boltzmann's distribution and the Gaussian approximate each other until there is a complete overlap on the optimum value of the fitness function. This demonstrates that the mean continuously moves to the best solutions and finally converges at the optimum value represented by the elite individual. Thus, the variance tends to zero because the optimum value has been found.

Additionally, in the same study,<sup>44</sup> the relationship between the Boltzmann distribution and the truncation method to find the optimum value is presented. In this case, two different optimization problems limited on the same range of variables and truncation values have been used.

First, it was observed that the truncation makes possible the approximation of the mean toward the optimum value of the fitness function in both cases. However, it is important to note that the problem with a single optimum undergoes an approximation that is faster than that of the problem with multiple local optima. This last behavior is promoted by the Boltzmann distribution because the Boltzmann distribution gets the information about the landscape of the function. In this case, the BUMDA algorithm is capable of perceiving that a more intense exploration must take place in the problem with multiple local optima. Therefore, the variance for this problem is larger than the corresponding variance of the problem with a single optimum.

Through this discussion is revealed that the performing characteristics of the BUMDA algorithm are given by the Boltzmann distribution and the truncation method. The former

meets the landscape of the function, and the latter leads the convergence.

On the basis of this analysis, it is evident that the BUMDA algorithm obtains the optimal solution using low computational effort. In addition, it is important to mention that the main parameter given by the user is the population size.

**2.4. Flow Sheet of the BUMDA Algorithm.** The flow sheet observed in Figure 6 shows that after the population ( $P_0$ )

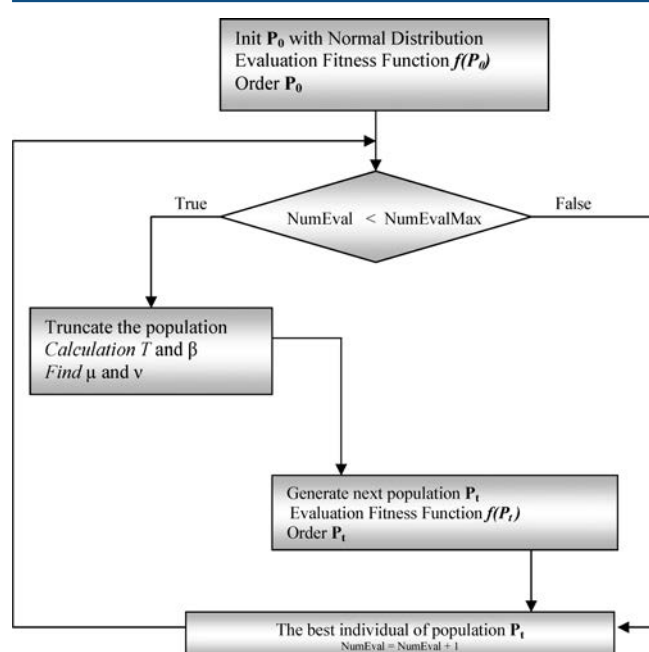


Figure 6. Flow sheet of the BUMDA algorithm.

is generated by using a normal distribution, it is evaluated [ $f(P_0)$ ] and enters the cycle if proposed. The optimization process is executed if the current function evaluations number (NumEval) is less than the maximum value established (NumEvalMax).

Along the optimization process, the population is truncated and the parameters ( $T$ ,  $\beta$ ) are internally calculated.  $\mu$  and  $\nu$  are determined with the respective equations. Thus, the new generation ( $P_t$ ) is produced by the model  $Q(x,t)$  in a quantity of the population size less 1. One individual is suppressed in order to add the best individual (elite individual) in each generation, thus preserving the size of the population. Also, it is important to mention that when the variance is larger than the value proposed, the new population will be produced using the model  $Q(x,t)$ . Otherwise, the exploration is reinitialized and each new individual will be generated as in the beginning, considering all the search range.

**2.5. Particular Considerations.** In the original context, the BUMDA algorithm was developed to optimize problems on continuous domains, not constrained. Nonetheless, problems in chemical engineering are modeled by multiple variables (continuous and discrete) and constraints that must be met. Therefore, to optimize this kind of problem using optimization tools under intensified searches, this algorithm has undergone some important settings:

1. Implementation of a method for handling of constraints.
2. Use of both continuous and discrete variables.
3. Inclusion of a reset mechanism.

In particular, there are two goals pursued by the reset mechanism: (a) explore intensively the search space and (b) reduce the possibility of remaining at local optima.

### 3. CASE STUDY

The case studies used here are shown in Table 1. The first of them is a mixture of alcohols (isomers), and the others are two

Table 1. Case Study

mixture	thermodynamic model
M1 ( <i>n</i> -butanol/isobutanol)	NRTL
M2 ( <i>n</i> -heptane/cyclohexane)	Chao–Seader
M3 (benzene/toluene)	Chao–Seader

hydrocarbon mixtures. The range of relative volatility varies from 1.44 to 2.4. Note that the thermodynamic model of Chao–Seader is used to simulate the hydrocarbon mixtures, whereas the NRTL model was applied to model the mixture of isomers. These thermodynamic models have been recommended<sup>46</sup> to handle hydrocarbon mixtures (Chao–Seader) and polar mixtures (NRTL) in the respective cases.

For the three case studies, a feed rate of 100 kmol/h as saturated liquid was used, with a composition of 50% mol. The purity and recovery targets are  $\approx 99.5\%$  mol. Likewise, a value of  $\Delta T_{i-\min}$  SR-SS of 3 °F as the minimum temperature driving force for energy integration between columns was established. On the other side, the minimum value of the compression ratio between the columns was defined as 1.1, considering a pressure drop of 0.3 kPa by stage. Finally, the limits of the design variables can be seen in Table 2.

Table 2. Limits of the Design Variables of HiDiC Sequences

mixture	reflux ratio (RR)	compression ratio (CR)	total stage number (NT)
M1	1.5–20	1.1–10	48–88
M2	1.5–20	1.1–10	28–68
M3	1.5–20	1.1–10	20–60

The limits of the number of stages were established taking into account the influence of this variable in the energy consumption and the economy of the HiDiC columns. It was done analyzing results obtained in other studies to split mixtures with similar characteristics.<sup>17,32,47</sup> Such studies show that the best values for the energy consumption and the TAC are found around the middle part in a range of two to three times the lower limit of the number of stages. Consequently, in this work, the upper limit for the number of stages was defined to be a value around two or three times the lower limit of the number of stages established. In this study, the lower limit was obtained through the short-cut method of Fenske–Underwood–Gilliland in Aspen Plus.

The limits of the reflux ratio were established as follows:

1. The simulation of the conventional column with the maximum number of stages (upper limit of the number of stages) and the simulation of the conventional design with the minimum number of stages (lower limit of the number of stages) were performed, and both purity and recovery were met.
2. The lower limit of RR was initially defined as the reflux ratio determined for the maximum stage number, and the

upper limit was established as the reflux ratio obtained for the design with the minimum number of stages.

3. A preliminary evaluation of several HIDiC designs was carried out considering these values, and their energetic and economic advantages were observed with several increments of RR on both limits. In this evaluation, it was found that using the RR values defined in point 2 did not result in the best benefits. Therefore, the limits used here represent the increased values that give a suitable relationship between the TAC and energy consumption.

In agreement with the design-optimization methodology here implemented, these limits are justified because RR has a strong relationship with the amount of energy to be integrated. In fact, this variable is considered to be the second most important variable in the design and optimization of HIDiC columns, only after the compression ratio.

Similarly, as has been observed in literature,<sup>32,48,35,47</sup> to obtain a proper balance between economy and energy savings in HIDiC sequences, the compression ratio is commonly found on values larger than 1 and less than 3. Nonetheless, to evaluate the capability of the BUMDA algorithm in terms of that variable (considered as the most important variable in the HIDiC columns), in this study an exploration range from 1.1 to 10 was defined. Through this consideration, valuable information will be obtained in relation to the efficacy of the algorithm to intensively explore regions of low compression ratios.

On the other hand, in this study, the HIDiC configuration without energy integration, shown in Figure 7, is considered to be a pseudo-conventional column, whereas the HIDiC sequence with energy integration, depicted in Figure 8, represents the general HIDiC.

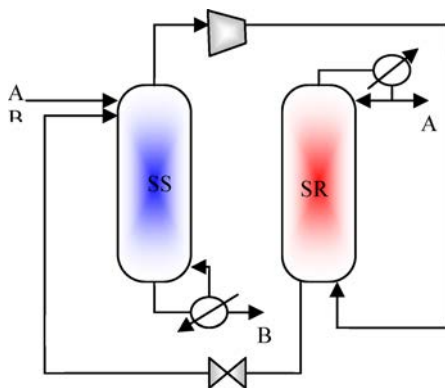


Figure 7. Conventional distillation sequence.

**3.1. Optimization Goals.** The optimization goal of the problem is the minimization of the total annual cost (TAC), as it is presented in eq 7. The optimization variables used in this study are the compression ratio, reflux ratio, and number of stages (NT).

The compression ratio and the reflux ratio represent the continuous optimization variables, while the number of stages denotes a discrete variable.

The problem's constraints are the recovery ( $x_{\text{recovery}}$ ) and purity ( $x_{\text{purity}}$ ) of the components, whose target is defined as  $\approx 0.995$  mol fraction. Also,  $3^\circ\text{F}$  is established as the minimum value of  $\Delta T_{\text{SR-SS}}$  for the energy integration and a pressure drop of 0.3 kPa by stage.

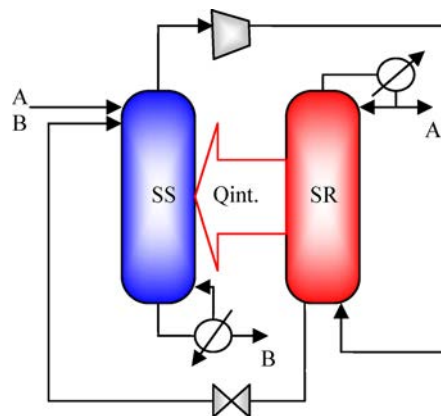


Figure 8. HIDiC distillation sequence.

$$\text{Min}(\text{TAC}) = f(\text{CR}, \text{RR}, \text{NT}) \quad (7)$$

Subject to

$$X_{\text{purity}} = X_{\text{recovery}} = 0.995 \pm \delta; \quad \delta = 0.0003; \quad \Delta T_{\text{SR-RR}} \geq 3^\circ\text{F}$$

where the  $\delta$  represents the tolerance allowed around the purity and recovery targets.

It is important to mention that eq 1 is treated here as a black box, and it is evaluated using Aspen Plus.

The three freedom degrees (optimization variables) used in this work were selected because they represent the main variables that define the performance of the HIDiC sequences. The importance of these variables is supported because through them it is possible to determinate the most convenient balance between economy and energy consumption. In other words, the combined effect of these variables denotes the feasibility, quantity, and quality of the energy integration in the HIDiC. In addition, despite the fact that the energy distribution was not established as an additional optimization variable, it is guessed that this variable is indirectly evaluated together with the thermal feasibility to integrate energy along the column.

Likewise, the value of delta was established as  $3 \times 10^{-4}$  in order to obtain a value close enough to 0.995 with reasonable computational effort to reach the convergence. The decision to select this value was supported when other values for delta ( $1 \times 10^{-4}$  and  $2 \times 10^{-4}$ ) were evaluated and whose results revealed that the computing effort to get convergence is considerably larger that required with the value of  $3 \times 10^{-4}$ .

**3.2. Methodology.** The procedure to optimize the HIDiC sequence starts with the design of the conventional column (Figure 1), which is divided into two symmetric columns ( $N_{\text{SR}} = N_{\text{SS}} = \text{NT}/2$ , Figure 7). Next, a compression ratio between the columns is established in such a way that SS is preserved at 1 atm while SR adopts a swing pressure (1.1–10 atm). Then this sequence is simulated in Aspen Plus, and  $\Delta T_{\text{SR-SS}}$  and the amount of heat to be integrated stage by stage ( $Q_i$ ) are determined. After that, the energy integration is carried out, and this HIDiC sequence (Figure 8) is simulated in Aspen Plus. In this way the set of constraints and the fitness function are evaluated.

Observe that in this work, both the conventional sequence and the HIDiC sequence have the same total number of stages. This was done to explore the behavior of these configurations by evaluating the energy distribution stage-by-stage at the same level as a first approach to using the BUMDA algorithm to optimize these sequences.

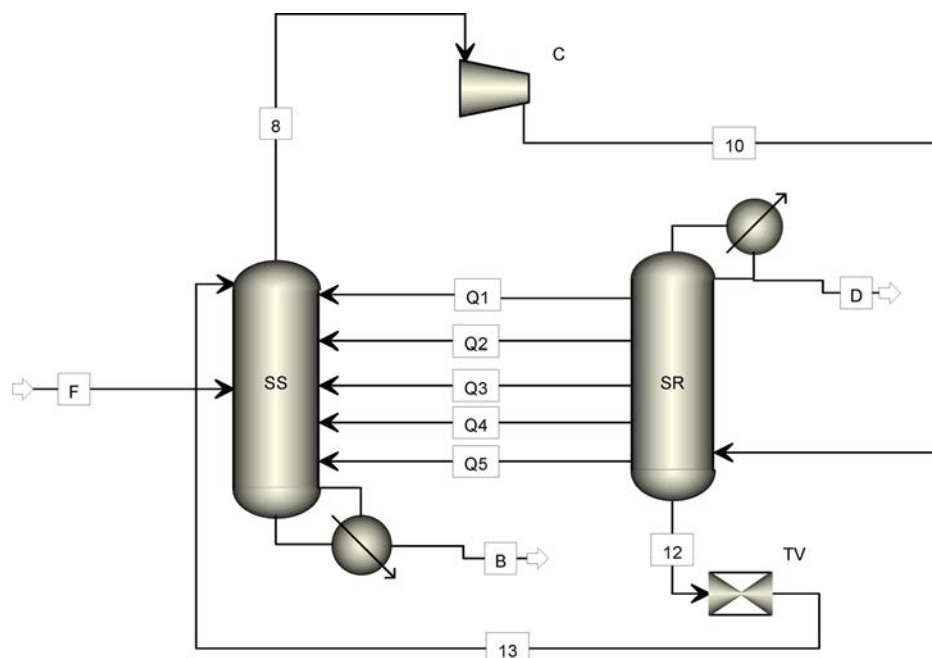


Figure 9. HIDiC configuration assembled in Aspen Plus.

On the other side, the energy integration is achieved in Aspen Plus using heat streams, which can be found in the block of streams of the simulator, together with the material and work streams. The heat streams ( $Q_i$ ) are drawn from the heat source (rectifying section) and are directed toward the corresponding heat sink (stripping section). Each heat stream transfers the amount of energy determined in the evaluation of the conventional column achieved in the previous step. Figure 9 shows schematically the implementation of the HIDiC configuration directly in the simulator.

In Figure 9, both the compressor (C) and the throttled valve (TV) make possible the change of pressure required between SR and SS.

The fitness function (TAC) represents the operation costs (COP) plus the capital costs (CC). The operation cost includes the heating steam, cooling water, and electricity. The capital costs involve the column shells, reboiler, condenser, compressor, and the heat-transfer area stage-by-stage. The transfer areas per stage ( $A_i$ ) and consequently the total area ( $A_t$ ) are determined in function of  $Q_i$  and  $\Delta T_i$  ( $\Delta T_{i,SR,SS}$ ) as is observed in eqs 8–10,<sup>35</sup> taking into consideration that in this case  $QT$  is the heat duty in the condenser of the rectifying section.

$$Q_i = \Delta T_i \left( \frac{QT}{\sum_{i=1}^n \Delta T_i} \right) \quad (8)$$

$$A_i = \left( \frac{Q_i}{U \Delta T_i} \right) \quad (9)$$

$$A_t = \sum_{i=1}^n A_i \quad (10)$$

where  $i$  is the corresponding stage and  $n$  is the number of stages with thermodynamic feasibility for performing the energy integration.

In this work, the overall heat-transfer coefficient to size the heat-transfer panels and reboilers was established as 200 Btu/

( $\text{h ft}^2 \text{ }^\circ\text{F}$ ); whereas the coefficient for the condenser was defined as 150 Btu/( $\text{h ft}^2 \text{ }^\circ\text{F}$ ). In the case of reboilers and condensers, these coefficients represent typical values for shell and tube exchangers.<sup>49</sup> Nevertheless, in literature<sup>24,31,35,47</sup> about the HIDiC sequences, similar values of  $U$  determined experimentally to design heat-transfer panels have been used.

As was shown in another study,<sup>27</sup> the panels can be structured like compact exchangers placed into the stripping section and open in the rectifying section. In this case, the steam from the rectifying section enters the panel and condenses; thereafter, liquid is returned to the rectifying section.

To obtain the total annual cost, Guthrie's method has been used,<sup>50</sup> considering low-pressure vapor and cooling water to environmental conditions, whose costs are 0.016 USD/kg and 0.0148 USD/ $\text{m}^3$ , respectively.<sup>49</sup> The electricity cost is 0.1 USD/kWh.<sup>51</sup>

The TAC is evaluated on a basis of 8000 operation hours per year. In addition, the evaluation of carbon dioxide emissions has been conducted using a model recently developed.<sup>52</sup> The thermodynamic efficiency ( $\eta$ ) was determined engaging a model based on considerations of the second law of the thermodynamic.<sup>46</sup> On the other side, to evaluate the total energy consumption and the  $\text{CO}_2$  emissions in the HIDiC sequence, the reboiler duty (QR) plus the compressor duty (Q comp) is considered.

The cost of the electricity used in this study was considered to be the widely employed value in the literature.<sup>35,49,48,47</sup> This value was selected to have conditions similar to those of other design and optimization strategies<sup>24,35,47</sup> with the goal of validating the methodology and determining the performance of the algorithm.

The resulting implementation for achieving the design and optimization is represented by the interface shown in Figure 10. In this interface, the BUMDA algorithm is the master algorithm programmed in Matlab, which invokes the Aspen Plus simulator through Excel to extract the design variables and evaluate the fitness function. The BUMDA algorithm uses a



Figure 10. Optimization interface.

constraint-handling method based on function penalization and the sum of constraint violations.

In this work, 60 individuals and 50 generations were used, resulting in 3000 function evaluations for each case study. The number of function evaluations used in this study represents the number in which a suitable value of the fitness is obtained using a reasonable computing time. This election took place after doing some evaluations considering several values (1800, 3000, and 3600).

On the other hand, this number of evaluations was considered to be the value of reference to intensively explore the search space. This intensive exploration is given by the reset mechanism, which is activated when the variance becomes lower than the value established.

In general terms, this fact means that the variance was used as an activator of the reset mechanism instead of being used as the stop criterion. This election leads to an intensive exploration of the search space, taking as a reference an appropriate number of function evaluations.

The simulations were made with a PC with an i5 processor core, clock frequency at 2.8 GHz, and 16 GB of RAM. On average, for each case study, 145 s were used for evaluation of the function.

#### 4. RESULTS

First, in agreement with the design and optimization goals established, it is important to highlight that the BUMDA algorithm has been able to successfully deal with complex problems (nonlinear and multivariable) constrained with efficacy and robustness through an intensified search using a reset mechanism.

The typical behavior of the fitness function in relation to the function evaluations number for the three case studies, presented in Figure 11, shows that as the function evaluations

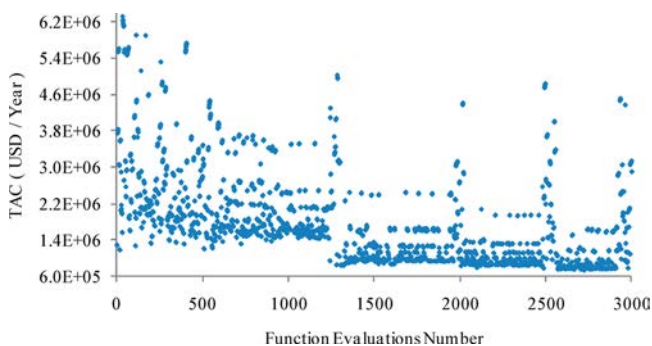


Figure 11. Behavior of the TAC with the function evaluations number.

number is increased, the fitness function (TAC) is continuously enhanced or kept on the best value found. The activation of the reset mechanism is observed by the sudden change of the fitness function after a uniform tendency. This means that the search space is reopening several times after a determined function evaluation. Notice that this mechanism is frequently activated after the first time, preserving the best solutions previously found and leading even to finding better values of

the TAC once again along the optimization process. This reflects the good performance of the BUMDA algorithm in leading the search toward the best solutions.

#### 4.1. Influence of the Compression Ratio on the TAC and the Energy Consumption of the HiDiC Sequences.

The common tendency found for the three case studies in terms of compression ratio can be observed in Figure 12. The

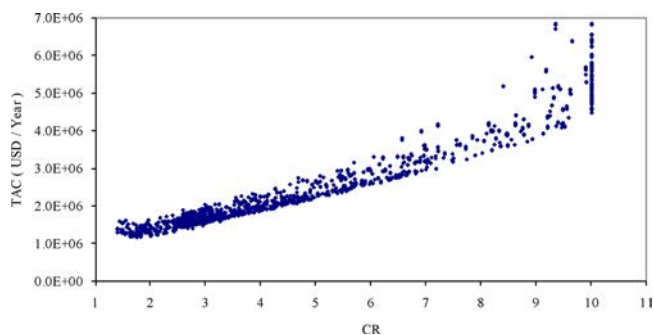


Figure 12. CR versus total annual cost.

analysis shows that as CR grows, the TAC is increased. This increase of the cost is generated because each kilowatt of electricity used in the compressor is more expensive than each kilowatt of heating steam provided in the reboiler. At the same time, the size of the compressor must be larger to compress higher vapor flows produced by energy integration at higher compression ratios. In addition, more internal exchangers (areas) must be placed to perform the heat integration between the columns. Furthermore, notice that the most profitable operation zone to preserve minor economical expenses is located on compression ratios among 1 and 2.5.

#### 4.2. Economic and Energetic Analysis of the HiDiC Sequences Compared with the Conventional Sequences.

In this part, the discussion considers some representative designs obtained for each case study. This selection was achieved taking as reference the TAC and the energy consumption simultaneously. Notice that each number of stages (NT) represents a HiDiC design. Furthermore, take into account that

$$\%Q = \frac{\text{reboiler duty of the HiDiC sequence}}{\text{reboiler duty of the conventional column}} \cdot 100$$

$$\%TAC = \frac{\text{TAC of the HiDiC sequence}}{\text{TAC of the conventional column}} \cdot 100$$

The terms represent the percentage of the energy consumption and the percentage of the TAC of the HiDiC column, respectively, in relation to that of the conventional sequence.

Considering the above and when an economic and energetic analysis on these representative designs is carried out, it is found that for the M1 case, observed in Figure 13, the cost of the HiDiC sequences is considerably comparable with that of the conventional column (even slightly lower, 2%) in several designs. However, for the M2 and M3 cases (shown in Figures 14 and 15, respectively), all HiDiC designs are more expensive than their conventional counterparts. Observe that the additional costs of the HiDiC designs represent between 30 and 68% for the M2 case and from 30 to 100% for the M3 case. The excess cost of the HiDiC in relation to that of the conventional column is due to the high cost of the heat-transfer

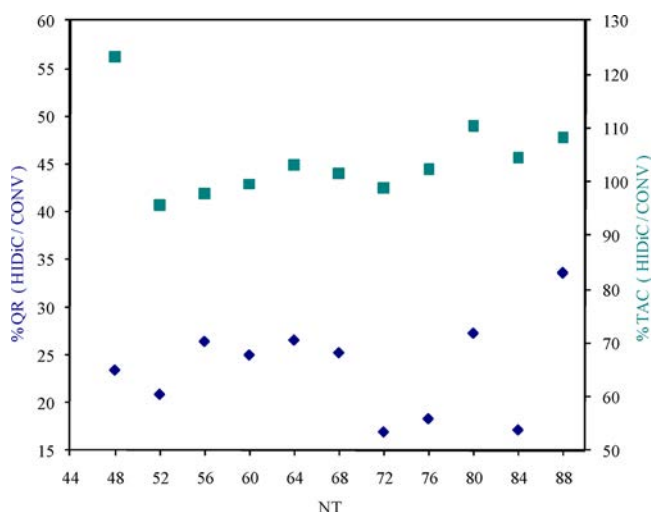


Figure 13. Total annual cost of HIDiC versus conventional; representative designs for M1.

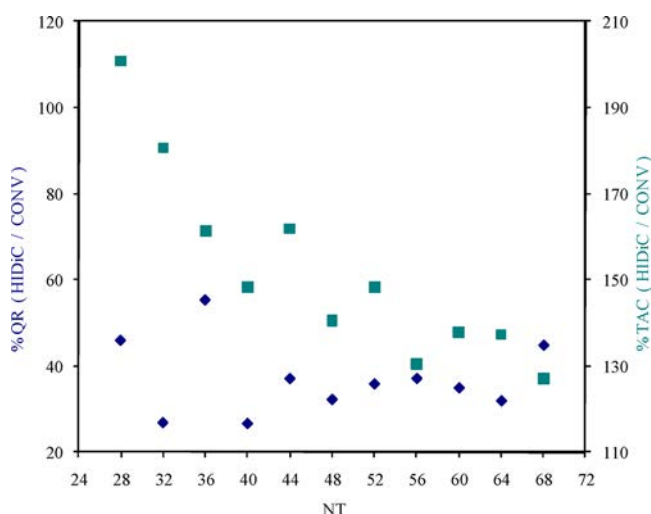


Figure 14. Total annual cost of HIDiC versus conventional; representative designs for M2.

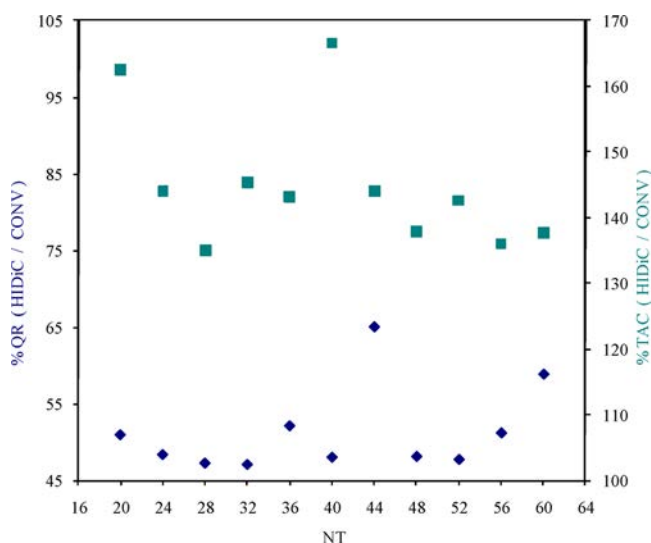


Figure 15. Total annual cost of HIDiC versus conventional; representative designs for M3.

area placed in the HIDiC columns and the capital cost of the compressor. In addition, the electricity to drive the compressor is several times more expensive than the heating steam. For this reason, a proper balance between the reduction of reboiler duty and the compression ratio selected to promote the energy integration must be found. At the same time, this excess of cost has a strong relationship with the characteristics of the mixtures to be separated. In this case, it is clear that the HIDiC offers more benefits when it is used to split a mixture of alcohols with low relative volatility than when it is used a mixture of hydrocarbons.

At the same time, when the energetic behavior is analyzed, the HIDiC configurations are able to significantly reduce the energy consumption in reference to the conventional column. For instance, in the M1 case, the energy savings oscillates between 55 and 84%. Similarly, M2 offers energy savings in a range of 40 to 75%; whereas for M3, the energy reduction is between 35 and 55%. These results represent the important reduction of carbon dioxide because of the direct relationship between carbon dioxide emissions and energy consumption.

#### 4.3. Internal Vapor and Liquid Flows of the HIDiC.

From another perspective, it is important to point out that the energy savings achieved by the HIDiC sequences are derived from the meaningful reductions of both the vapor flow produced in the reboiler (stripping section) and the flow of steam to be liquefied in the condenser (rectifying section) in relation to the conventional sequences. The generalized behavior for the three case studies is presented in Figure 16. The reduction for M1 represents around 92%, whereas for the M2 and M3 cases, the reductions achieved were approximately 70 and 50%, respectively.

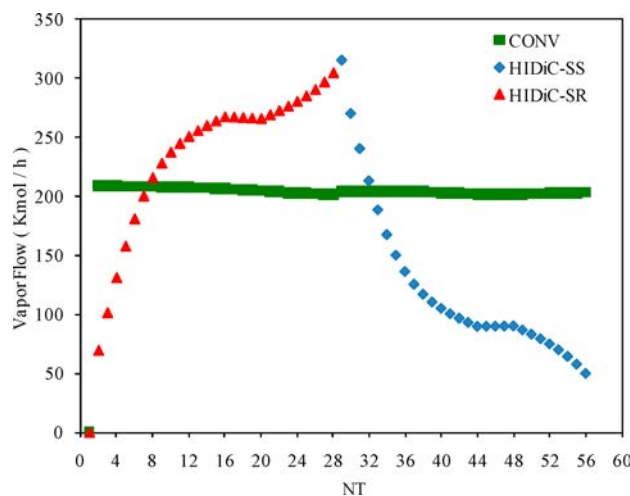


Figure 16. Vapor profiles for the HIDiC design versus its conventional counterpart.

#### 4.4. Relationship between the Operation Cost and the Capital Cost on the HIDiC Designs.

The analysis of the influence of the capital cost and operation cost on the TAC for the three case studies revealed that the capital cost is larger than the operation cost. In the M1 case, shown in Figure 17, it was determined that the capital cost contributes around 74% of the TAC. In an analogous analysis, it was found that the capital cost represents about 70% and 60% of the TAC for the M2 and M3 cases, respectively. This cost mainly represents the investment

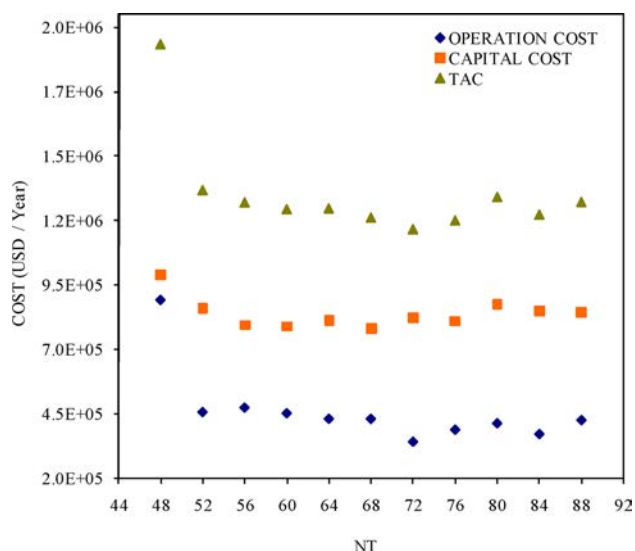


Figure 17. Analysis of costs of representative designs.

in the compressor and the heat-transfer areas as a result of the energy integration.

**4.5. Energy Distribution in the HiDiC Sequences.** With the aim of showing the energy distribution, in this section the best HiDiC designs have been selected for each case study. Here, the best HiDiC design is that design that presents the best balance between the TAC and energy savings.

First, it is worth mentioning that the energy distribution in the three case studies follows different patterns. Notice that in the M1 case (Table 3), the heat was distributed on all stages of the column, reflecting a complete thermodynamic feasibility between SR and SS. In this case, 5642 ft<sup>2</sup> were engaged to internally transfer 14 242 013.4 Btu/h. In addition, for the mixture M2, the energy distribution is located on 24 stages, leaving four stages in the middle part of the column without any energy integrating, integrating a total of 6 589 821.18 Btu/h, with a requirement of 2429 ft<sup>2</sup> of total area installed as internal heat exchangers (Table 4). Finally, in the M3 case (Table 5), the integrated energy was distributed on both extremes of the column, particularly in stages 2, 12, and 13, achieving integration of about 3 579 643 Btu/h, representing a total heat-transfer area of 1389 ft<sup>2</sup>.

**4.6. Economic and Energetic Analysis of the HiDiC Sequences Compared with the Conventional Sequences.** The summary results presented in Tables 6–8 illustrate the set of design parameters determined through the optimization process for each of the HiDiC designs selected in every case study. These results demonstrate that both the decision variables and constraints established were preserved in the defined range. Also notice that the HiDiC designs engage small reflux ratios (derived from the reductions of vapor and liquid condensate flows) compared with that of the conventional sequence. This leads to considerable energy savings as a result of a thermodynamic efficiency higher than that of the conventional sequences. This reveals that important energetic benefits are obtained while the TAC may be slightly lower than (mixture M1) or superior to (M2 and M3) the cost of the conventional configuration.

**4.7. Economic and Energetic Analysis of the Best HiDiC Sequence Compared with the Optimized Conventional Sequence.** In the previous discussion, the performance of the best HiDiC sequence in relation to its corresponding not

Table 3. Energy Distribution and Heat-Transfer Areas for the HiDiC Design with 72 Total Stages

stage	temperature (°F)		$\Delta T$ (°F)	heat duty (Btu/h)	A (ft <sup>2</sup> )
	SR	SS			
condenser	252.05	234.72	17.33	-2 052 334.20	490.30
2	252.19	235.47	16.72	589 770.84	176.64
3	252.31	236.25	16.06	574 291.40	179.14
4	252.42	237.05	15.37	556 926.02	181.42
5	252.54	237.84	14.7	537 729.00	183.31
6	252.6710	238.63	14.041	516 876.20	184.65
7	252.79	239.41	13.38	494 678.03	185.28
8	252.93	240.16	12.77	471 575.76	185.11
9	253.07	240.87	12.2	448 117.17	184.08
10	253.22	241.53	11.69	424 913.00	182.23
11	253.38	242.14	11.24	402 581.55	179.67
12	253.55	242.71	10.84	381 693.28	176.55
13	253.73	243.23	10.5	362 727.00	173.07
14	253.93	243.70	10.23	346 046.45	169.44
15	254.15	244.13	10.02	331 899.49	165.83
16	254.40	244.53	9.87	320 436.99	162.40
17	254.67	244.88	9.79	311 743.06	159.28
18	254.98	245.21	9.77	305 869.19	156.54
19	255.32	245.51	9.81	302 863.99	154.25
20	255.71	245.79	9.92	302 792.52	152.47
21	256.13	246.04	10.09	305 742.08	151.23
22	256.61	246.28	10.33	311 809.81	150.57
23	257.14	246.51	10.63	321 073.25	150.50
24	257.72	246.72	11	333 544.21	151.00
25	258.36	246.92	11.44	349 112.73	152.03
26	259.05	247.12	11.93	367 495.23	153.46
27	259.76	247.31	12.45	388 203.48	155.17
28	260.51	247.49	13.02	410 552.61	157.00
29	261.27	247.66	13.61	433 716.32	158.70
30	262.04	247.83	14.21	456 820.00	160.19
31	262.79	247.99	14.8	479 048.41	161.36
32	263.52	248.16	15.36	499 736.21	162.13
33	264.23	248.32	15.91	518 421.14	162.50
34	264.89	248.47	16.42	534 852.70	162.51
35	265.52	248.63	16.89	548 966.60	162.20
reboiler	266.11	248.78	17.33	989 506.93	75.40

optimized conventional column was analyzed (best HiDiC/not optimized conv.).

In this section, the discussion will be on the behavior between the best HiDiC sequence and the best optimized conventional column (best HiDiC/best optimized conv.). At the same time, the results between (best HiDiC/not optimized conv.) and (best HiDiC/best optimized conv.) will be compared.

First, as can be seen in Table 9, the optimized conventional design for the separation of mixtures M1 and M2 have eight more stages than the best HiDiC sequence. Nevertheless, for the mixture M3 the best optimized conventional column has four stages less than the best HiDiC. Furthermore, the TAC of the best HiDiC for M1 is again slightly less than the TAC of the best optimized conventional column (0.33%). Similarly, the TAC for the best HiDiC design is once more superior to the TAC of the best optimized conventional design for M2 (30.7%) and M3 (36.26%). On the other hand, a considerable energy savings is achieved for M1 (82.4%), followed by M2 (64.6%) and M3 (50.65%).

**Table 4. Energy Distribution and Heat-Transfer Areas for the HIDiC Design with 56 Total Stages**

stage	temperature (°F)		$\Delta T$ (°F)	heat duty (Btu/h)	A (ft <sup>2</sup> )
	SR	SS			
condenser	216.44	192.77	23.67	-1 860 117.8	465.00
2	216.62	194.91	21.71	860 896.60	198.30
3	216.78	197.10	19.68	799 475.12	203.16
4	216.94	199.25	17.69	720 139.6	203.48
5	217.11	201.26	15.85	624 929.14	197.03
6	217.30	203.07	14.22	520 923.8	183.10
7	217.50	204.68	12.82	418 783.2	163.29
8	217.71	206.07	11.64	328 594.06	141.11
9	217.95	207.28	10.66	256 128.81	120.10
10	218.20	208.34	9.86	202 132.68	102.51
11	218.48	209.28	9.20	164 062.8	89.10
12	218.80	210.11	8.69	138 232.83	79.53
13	219.14	210.85	8.29	121 182.65	73.01
14	219.54	211.51	8.03	110 211.8	68.65
15	219.98	212.11	7.87	103 427.36	65.70
16	-	-	-	-	0
17	-	-	-	-	0
18	-	-	-	-	0
19	-	-	-	-	0
20	223.17	214.61	8.56	104 414.85	60.98
21	224.05	215.02	9.03	110 654.14	61.27
22	225.04	215.40	9.64	119 619.43	62.10
23	226.13	215.75	10.38	131 991.96	63.62
24	227.32	216.08	11.24	148 648.16	66.13
25	228.60	216.39	12.21	170 652.68	70.00
26	229.96	216.68	13.28	199 207.40	75.00
27	231.37	216.96	14.41	235 512.05	81.72
reboiler	232.81	217.24	15.57	1 455 282.31	121.20

**Table 5. Energy Distribution and Heat-Transfer Areas for the HIDiC Design with 28 Total Stages**

stage	temperature (°F)		$\Delta T$ (°F)	heat duty (Btu/h)	A (ft <sup>2</sup> )
	SR	SS			
condenser	223.86	202.19	21.67	-1 692 527.73	522.64
2	224.25	207.54	16.70	1 902 988.69	569.47
-	-	-	-	-	-
12	240.74	232.16	8.57	561 537.63	327.15
13	244.09	232.77	11.32	1 115 117.32	492.40
reboiler	248.94	233.20	15.74	1 379 565.67	115.00

**Table 6. Design Variables of the Best HIDiC Sequence Described and Its Conventional Counterpart (Mixture M1)**

	conventional	HIDiC
NT	72	72
RR	5.27	0.084
CR	1/1	1.76/1
recovery	0.9952	0.9952
purity	0.9951	0.9950
QR (Btu/h)	15 000 000	989 506.93
QComp. (Btu/h)	-	1 094 252.25
Q int. (Btu/h)	-	14 242 625.7
At (ft <sup>2</sup> )	-	5642
$\eta$	3.2	32.9
CO <sub>2</sub> (ton/year)	8576	1190.3
TAC (USD/year)	1 348 035	1 164 210

**Table 7. Design Variables of the Best HIDiC Sequence Described and Its Conventional Counterpart (Mixture M2)**

	conventional	HIDiC
NT	56	56
RR	3.06	0.382
CR	1/1	1.862/1
recovery	0.9951	0.9949
purity	0.9951	0.9949
QR (Btu/h)	5 810 677.62	1 455 282.31
QComp. (Btu/h)	-	700 806.67
Q int. (Btu/h)	-	6 589 821.18
At (ft <sup>2</sup> )	-	2429
$\eta$	14.0007	46.0025
CO <sub>2</sub> (ton/year)	3206.93	1187.79
TAC (USD/year)	615 717.60	803 937.05

**Table 8. Design Variables of the Best HIDiC Sequence Described and Its Conventional Counterpart (Mixture M3)**

	conventional	HIDiC
NT	28	28
RR	1.675	0.221
CR	1/1	2.147/1
recovery	0.9949	0.9949
purity	0.9949	0.9949
QR (Btu/h)	4 150 319.44	1 379 565.67
QComp. (Btu/h)	-	577 626.011
Q int. (Btu/h)	-	3 579 643.65
At (ft <sup>2</sup> )	-	1389
$\eta$	16.4859	48.74
CO <sub>2</sub> (Ton/Year)	2371.16	1108.30
TAC (USD/Year)	393 400	531 022

**Table 9. Best HIDiC versus Not Optimized Conventional Column and Optimized Conventional Column**

	best HIDiC/optimized conv.			best HIDiC/not optimized conv.			best HIDiC
	%Q	%TAC	NT	%Q	%TAC	NT	NT
M1	17.60	99.67	80	16.91	98.90	72	72
M2	35.40	130.70	48	37.11	130.57	56	56
M3	49.35	136.26	32	47.16	134.98	28	28

The degree of similitude of the results obtained between (best HIDiC/best optimized conv.) and (best HIDiC/not optimized conv.) shown in Table 9 indicates that the intensified search guided by the BUMDA algorithm and the truncation method is concentrated on the space where the best solutions can be found. This obeys the fundamentals of the BUMDA algorithm.

## 5. CONCLUSIONS

In this work, the design and optimization of the HIDiC configurations was developed using a constrained stochastic algorithm based on Boltzmann's distribution and attached with a reset mechanism. Moreover, in this robust methodology, the reflux ratio is included as a new optimization variable. The process was performed by the Matlab-Excel-Aspen Plus interface, using the rigorous model Radfrac to perform the simulations in Aspen Plus.

Results demonstrated that the BUMDA algorithm was able to track the problem involving both continuous (reflux ratio) and discrete (compression ratio and number of stages)

variables. Thus, the economic and energetic issues around the HIDiC configurations were determined.

In energetic terms, the benefits that the HIDiC configurations are able to offer were ratified. For instance, the energy savings achieved by the best HIDiC design of M1 was approximately 84%, whereas the energy savings obtained for the best HIDiC designs in the M2 and M3 cases were 62.5% and 52.5%, respectively.

The importance of the reflux ratio as optimization ratio is shown in the energy savings because that contributes in an important way to the determination of the amount of energy available in the source to be integrated.

Additionally, it is clear that the TAC of HIDiC sequence is less (2%) than the TAC of the conventional column for the best HIDiC design in the mixture M1. However, the TAC of the HIDiC sequence is larger than the TAC of the conventional column in the best HIDiC designs of the systems M2 (32%) and M3 (35%). Therefore, it is determined that as the difficulty of separation of the mixture is increased, both the TAC and energy savings are enhanced.

Likewise, through the similitude of the comparative results of the best HIDiC before and after the optimization of the conventional column, the strength of the optimization strategy is proven.

Considering these results, it is demonstrated that the Boltzmann and truncation methods lead to establishing the search in the best region, but an exhaustive exploration is promoted by the reset mechanism.

## AUTHOR INFORMATION

### Corresponding Author

\*E-mail: gsegovia@ugto.mx.

### Notes

The authors declare no competing financial interest.

## REFERENCES

- (1) Engelen, H. K.; Skogestad, S. Selecting appropriate control variables for a heat integrated distillation system with prefractionator. *Comput. Chem. Eng.* **2004**, *28*, 683–691.
- (2) Humphrey, J. L.; Siebert, A. F. Separation technologies: an opportunity for energy savings. *Chem. Eng. Prog.* **1992**, *10*, 92–98.
- (3) De Koeijer, G. M.; Kjelstrup, S. Minimizing entropy production rate in binary tray distillation. *Int. J. Appl. Thermodyn.* **2000**, *3*, 105–110.
- (4) Humphrey, J. L.; Siebert, A. F.; Koort, R. A. *Separation technologies: Advances and priorities*. US Department of Energy, Office of Industrial Technologies: Washington, DC, 1991.
- (5) Null, H. R. Heat pumps in distillation. *Chem. Eng. Prog.* **1976**, *73*, 58–64.
- (6) Finelt, S. Better C3 distillation pressure. *Hydrocarbon Process. (1966-2001)* **1979**, *58*, 95–98.
- (7) Menzies, M. A.; Johnson, A. I. Steady-state modeling and parametric study of a vapor recompression unit. *Can. J. Chem. Eng.* **1981**, *59*, 487–491.
- (8) Meili, A. Heat pumps for distillation columns. *Chem. Eng. Prog.* **1990**, *60*–65.
- (9) Al-Elg, A. H.; Palazoglu, A. Modeling and control of a high-purity double-effect distillation column. *Comput. Chem. Eng.* **1989**, *13*, 1183–1187.
- (10) Han, M.; Park, S. Multivariable control of double-effect distillation configurations. *J. Process Control* **1996**, *6*, 247–253.
- (11) Hasebe, S.; Noda, M.; Hashimoto, I. Optimal operation policy for total reflux and multi-effect batch distillation systems. *Comput. Chem. Eng.* **1999**, *23*, 523–532.
- (12) Ophir, A.; Gendel, A. Adaptation of the multi-effect distillation (MED) process to yield high purity distillate for utilities, refineries and chemical industry. *Desalination* **1994**, *98*, 383–390.
- (13) Petlyuk, F. B.; Platonoy, V. M.; Slavinskii, D. M. Thermodynamically optimal method for separating multicomponent mixtures. *Int. Chem. Eng.* **1965**, *5*, 555–561.
- (14) Nakaiwa, M.; Huang, K.; Owa, M.; Akiya, T.; Nakane, T.; Sato, M.; Takamatsu, T. Energy savings in heat-integrated distillation columns. *Energy* **1997**, *22*, 621–625.
- (15) Nakaiwa, M.; Huang, K.; Naito, K.; Endo, A.; Owa, M.; Akiya, T.; Nakane, T.; Takamatsu, T. A new configuration of ideal heat integrated distillation columns (HIDiC). *Comput. Chem. Eng.* **2000**, *24*, 239–245.
- (16) Olujic, Z.; Fakhri, F.; De Rijke, A.; De Graauw, J.; Jansens, P. J. Internal heat integration—The key to an energy conserving distillation column. *J. Chem. Technol. Biotechnol.* **2003**, *78*, 241–248.
- (17) Huang, K.; Shan, L.; Zhu, Q.; Qian, J. A totally heat-integrated distillation column (THIDiC) – The effect of feed pre-heating by distillate. *Appl. Therm. Eng.* **2008**, *28*, 856–864.
- (18) Jana, A. K. Heat integrated distillation operation. *Appl. Energy* **2009**, *1*–18.
- (19) Mah, R. S. H.; Nicholas, J. J.; Wodnik, R. B. Distillation with secondary reflux and vaporization: A comparative evaluation. *AIChE J.* **1977**, *23*, 651–657.
- (20) Govind, R. Distillation column and process. US Patent, 4,615,770, 1986.
- (21) Govind, R. Dual distillation columns. US Patent, 4,681,661, 1987.
- (22) Glenchur, T.; Govind, R. Study on a continuous heat integrated distillation column. *Sep. Sci. Technol.* **1987**, *22*, 2323–2338.
- (23) Naito, K.; Nakaiwa, M.; Huang, K.; Endo, A.; Aso, K.; Nakanishi, T.; Noda, H.; Takamatsu, T. Operation of a bench-scale ideal heat integrated distillation column (HIDiC): An experimental study. *Comput. Chem. Eng.* **2000**, *24*, 495–499.
- (24) Nakaiwa, M.; Huang, K.; Endo, A.; Ohmori, T.; Akiya, T.; Takamatsu, T. Internally heat-integrated distillation columns: A review. *Chem. Eng. Res. Des.* **2003**, *81*, 162–177.
- (25) Roffel, B.; Betlem, B. H. L.; De Ruijter, J. A. F. First principles dynamic modeling and multivariable control of a cryogenic distillation process. *Comput. Chem. Eng.* **2000**, *24*, 111–123.
- (26) Sun, L.; Olujic, Z.; De Rijke, A.; Jansens, P. J. Industrially viable configurations for a heat-integrated distillation column, better processes for bigger profits. *Proceedings of 5th International Conference on Process Intensification for the Chemical Industry*, Maastricht, The Netherlands, October 13–15, 2003, .
- (27) De Graauw, J.; Steenbakker, M. J.; De Rijke, A.; Olujic, Z.; Jansens, P. J. Distillation column with heat integration. Dutch Patent, P56921NL00, 2003.
- (28) Schmal, J. P.; Van Der Kooij, H. J.; De Rijke, A.; Olujic, Z.; Jansens, P. J. Internal versus external heat integration: Operational and economical analysis. *Chem. Eng. Res. Des.* **2006**, *84*, 374–380.
- (29) Fukushima, T.; Kano, M.; Hasebe, S. Dynamics and control of heat integrated distillation column (HIDiC). *J. Chem. Eng. Jpn.* **2006**, *39*, 1096–1103.
- (30) Huang, K.; Shan, L.; Zhu, Q.; Qian, J. Design and control of an ideal heat-integrated distillation column (ideal HIDiC) system separating a close-boiling ternary mixture. *Energy* **2007**, *32*, 2148–2156.
- (31) Gadalla, M.; Jiménez, L.; Olujic, Z.; Jansens, P. J. A thermo-hydraulic approach to conceptual design of an internally heat-integrated distillation column (i-HIDiC). *Comput. Chem. Eng.* **2007**, *31*, 1346–1354.
- (32) Iwakabe, K.; Nakaiwa, M.; Huang, K.; Nakanishi, T.; Røsjorde, A.; Ohmori, T. Performance of an internally heat-integrated distillation column (HIDiC) in separation of ternary mixtures. *J. Chem. Eng. Jpn.* **2006**, *39*, 417–425.
- (33) Abushwiref, F.; Elakrami, H.; Emtir, M. Recovery of aromatics from pyrolysis gasoline by conventional and energy-integrated extractive distillation. *Comput.-Aided Chem. Eng.* **2007**, *24*, 1071–1076.

- (34) Cabrera-Ruiz, J. Design and optimization of internal energy integrating columns using the grand composite curve (GCC). MS Thesis, 2009; pp 41–59.
- (35) Suphanit, B. Design of internally heat-integrated distillation column (HIDiC): Uniform heat transfer area versus uniform heat distribution. *Energy* **2010**, *35*, 1505–1514.
- (36) Harwardt, A.; Kraemer, K.; Marquardt, W. Identifying optimal mixture properties for HIDiC application. *Proceedings of Distillation and Absorption* **2010**.
- (37) Andrecovich, M. J.; Westerberg, A. W. A MILP Formulation for Heat-Integrated Distillation Sequence Synthesis. *AIChE J.* **1985**, *31*, 1461.
- (38) Paules, G. E., IV; Floudas, C. A. A Mixed-Integer Nonlinear Programming Formulation for the Synthesis of Heat-Integrated Distillation Sequences. *Comput. Chem. Eng.* **1990**, *4*, 1397.
- (39) Smith, E. M. B.; Pantelides, C. C. Design of Reaction/Separation Networks using Detailed Models. *Comput. Chem. Eng.* **1995**, *19*, S83.
- (40) Caballero, J. A.; Grossmann, I. E. Aggregated Models for Integrated Distillation Systems. *Ind. Eng. Chem. Res.* **1999**, *38*, 2330.
- (41) Gutiérrez-Antonio, C.; Briones-Ramírez, A. Pareto Front of Ideal Petlyuk Sequences Using a Multiobjective Genetic Algorithm with Constraints. *Comput. Chem. Eng.* **2009**, *33*, 454.
- (42) Vázquez-Ojeda, M.; Segovia-Hernández, J. G.; Hernández, S.; Hernández-Aguirre, A.; Kiss, A. A. Design and Optimization of an Ethanol Dehydration Process Using Stochastic Methods. *Sep. Purif. Technol.* **2013**, *105*, 90–97.
- (43) Miranda-Galindo, E. Y.; Segovia-Hernández, J. G.; Hernández, S.; Gutiérrez-Antonio, C.; Briones-Ramírez, A. Reactive Thermally Coupled Distillation Sequences: Pareto Front. *Ind. Eng. Chem. Res.* **2011**, *50*, 926–938.
- (44) Valdez, S. I.; Hernandez, A.; Botello, S. A Boltzmann based estimation of distribution algorithm. *Inf. Sci. (New York)* **2013**, *236*, 126–137.
- (45) Cortez-González, J.; Murrieta-Dueñas, R.; Gutiérrez-Guerra, R.; Segovia - Hernández, J. G.; Hernández- Aguirre, A. Design and optimization of pressure swing distillation using a stochastic algorithm based in the Boltzmann distribution. *Proceedings of European Symposium on Computer Aided Process Engineering - 22 (ESCAPE)*, 2012; pp 687–691.
- (46) Seader, J. D.; Henley, E. *Separation Process Principles*; John Wiley and Sons: New York, 2006.
- (47) Lianghua, X.; Xigang, Y.; Dawei, C.; Yiqing, L.; Kuotsung, Y. Reversibility Analysis for Design Optimization of an Internally Heat-Integrated Distillation. *Chem. Eng. Technol.* **2013**, *36*, 1147–1156.
- (48) Olujic, Z.; Sun, L.; de Rijke, A.; Jansens, P. J. Conceptual design of an internally heat integrated propylene-propane splitter. *Energy* **2006**, *31*, 383–3096.
- (49) Turton, R.; Bailie, C. R.; Whiting, B. W.; Shaewitz, A. J. *Analysis, Synthesis, and Design of Chemical Processes*. Prentice Hall: Upper Saddle River, NJ, 2004; Appendix A.
- (50) Guthrie, K. M. *Process Estimating Evaluation and Control*; Craftsman Book Co.: Solana Beach, CA, 1974.
- (51) Nakaiwa, M.; Huang, K.; Naito, K.; Endo, A.; Akiya, T.; Akiya, T.; Nakane, T.; Takamatsu, T. Parameter analysis and optimization of ideal heat integrated distillation columns. *Comput. Chem. Eng.* **2001**, *25*, 737–744.
- (52) Gadalla, M. A.; Olujic, Z.; Jansens, P. J.; Jobson, M.; Smith, R. Reducing CO<sub>2</sub> emissions and energy consumption of heat-integrated distillation systems. *Environ. Sci. Technol.* **2005**, *39*, 6860–6870.